Hindawi Publishing Corporation
Advances in High Energy Physics
Volume 2013, Article ID 217858, 14 pages
http://dx.doi.org/10.1155/2013/217858

Research Article

$X(1870)$ and $\eta_2(1870)$: Which Can Be Assigned as a Hybrid State?

Bing Chen,[1] Ke-Wei Wei,[1] and Ailin Zhang[2]

[1] *School of Physics and Electrical Engineering, Anyang Normal University, Anyang 455000, China*
[2] *Department of Physics, Shanghai University, Shanghai 200444, China*

Correspondence should be addressed to Bing Chen; chenbing@shu.edu.cn

Received 11 July 2013; Revised 15 September 2013; Accepted 23 September 2013

Academic Editor: Gongnan Xie

The mass spectrum and strong decays of the $X(1870)$ and $\eta_2(1870)$ are analyzed. Our results indicate that $X(1870)$ and $\eta_2(1870)$ are the two different resonances. The narrower $X(1870)$ seems likely a good hybrid candidate. We support the $\eta_2(1870)$ as the $\eta_2(2^1D_2)$ quarkonium. We suggest to search the isospin partner of $X(1870)$ in the channels of $J/\psi \longrightarrow \rho f_0(980)\pi$ and $J/\psi \longrightarrow \rho b_1(1235)\pi$ in the future. The latter channel is very important for testing the hybrid scenario.

1. Introduction

An isoscalar resonant structure of $X(1870)$ was observed by the BESIII Collaboration with a statistical significance of 7.2σ in the processes $J/\psi \to \omega X(1870) \to \omega\eta\pi^+\pi^-$ recently [1]. Its mass and width were given as

$$M = 1877.3 \pm 6.3^{+3.4}_{-7.4}\,\text{MeV}, \qquad \Gamma = 57 \pm 12^{+19}_{-4}\,\text{MeV}. \quad (1)$$

Here the first errors are statistical and the second ones are systematic. The product branching fraction of $\mathscr{B}(J/\psi \to \omega X(1870)) \cdot \mathscr{B}(X(1870) \to a_0^{\pm}(980)\pi^{\mp}) \cdot \mathscr{B}(a_0^{\pm}(980) \to \eta\pi^{\pm}) = [1.5 \pm 0.26(\text{stat})^{+0.72}_{-0.36}(\text{syst})] \times 10^{-4}$ was also presented [1]. But the quantum numbers of $X(1870)$ are still unknown, then the partial wave analysis is required in future.

The mass of $X(1870)$ is consistent with the $\eta_2(1870)$, but the width is much narrower than the $\eta_2(1870)$. In the tables of the Particle Data Group (PDG) [2], the available mass and width of $\eta_2(1870)$ are

$$M = 1842 \pm 8\,\text{MeV}, \qquad \Gamma = 225 \pm 14\,\text{MeV}. \quad (2)$$

The $\eta_2(1870)$ has been observed in $\gamma\gamma$ reactions [3, 4], $p\overline{p}$ annihilation [5–8], and radiative J/ψ decays [9]. It should be stressed that radiative J/ψ decay channels (Figure 1(a)) and $p\overline{p}$ annihilation processes are the ideal glueball hunting grounds. But the glueball production is suppressed in $\gamma\gamma$ reaction. By contrast, the hadronic J/ψ decay are considered "hybrid rich" (Figure 1(b)).

Furthermore, the branching ratio $\mathscr{R}_1 = \Gamma(\eta_2(1870) \to a_2(1320)\pi)/\Gamma(\eta_2(1870) \to a_0(980)\pi) = 32.6 \pm 12.6$ reported by the WA102 Collaboration indicates that the decay channel of $a_0(980)\pi$ is tiny for $\eta_2(1870)$ [7]. This has been confirmed by an extensive reanalysis of the Crystal Barrel data [10]. Differently, the analysis of BESIII Collaboration indicates that the $X(1870)$ primarily decays via the $a_0(980)\pi$ channel [1]. Then the present measurements of the decay widths, productions, and decay properties suggest that $\eta_2(1870)$ and $X(1870)$ are two different isoscalar mesons.

If the production process $J/\psi \to \omega X(1870)$ is mainly hadronic, the quantum numbers of $X(1870)$ should be 0^+0^{-+}, 0^+1^{++}, or 0^+2^{-+}. One notices that the predicted masses for the light 0^+0^{-+}, 0^+1^{++} and 0^+2^{-+} hybrids overlap 1.8 GeV in the Bag model [11, 12], the flux tube model [13, 14], and the constituent gluon model [15]. In addition, the decay width of isoscalar 2^{-+} hybrid is expected to be narrow [16]. Therefore, $X(1870)$ becomes a possible 2^{-+} hybrid candidate.

In addition, the predicted masses of 0^{-+} and 2^{-+} glueball are much higher than 1.8 GeV by lattice gauge theory [17–19]. Therefore, $X(1870)$ is not likely to be a glueball state. Moreover, the molecule and four-quark states are not expected in this region [16]. Then the unclear structure $X(1870)$ looks more like a good hybrid candidate. But the actual situation

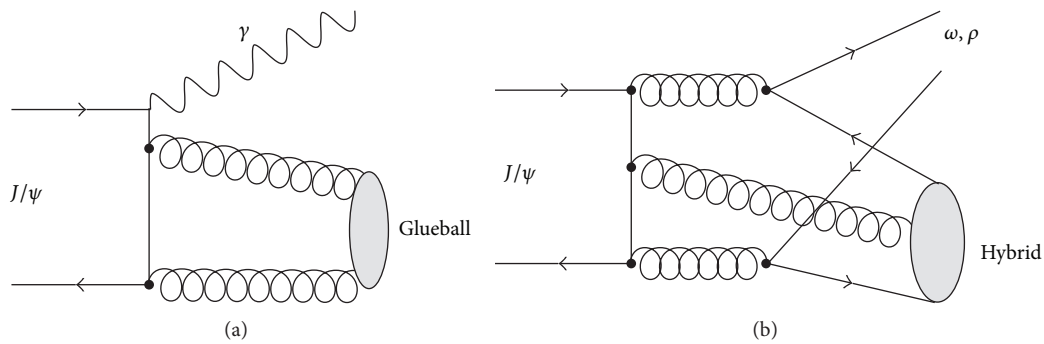

Figure 1: (a) A prior production of glueball in the $J/\psi \to \gamma X_G$; (b) a prior production of hybrid in the $J/\psi \to \omega X_H$.

is much complicated because the nature of $\eta_2(1870)$ is still ambiguous.

(i) Since no lines of evidence have been found in the decay mode of $K\overline{K}\pi$, the $\eta_2(1870)$ disfavors the $1^1D_2 s\bar{s}$ quarkonium assignment. The mass of $\eta_2(1870)$ seems much smaller for the $2^1D_2 n\bar{n}$ ($n\bar{n} \equiv (u\bar{u} + d\bar{d})/\sqrt{2}$) state in the Godfrey-Isgur (GI) quark model [20]. Therefore the $\eta_2(1870)$ has been assigned as the 2^{-+} hybrid state [10, 21–23].

(ii) However, Li and Wang pointed out that the mass, production, total decay width, and decay pattern of the $\eta_2(1870)$ do not appear to contradict with the picture of it as being the conventional $2^1D_2 n\bar{n}$ state [24].

Therefore, systematical study of the mass spectrum and strong decay properties is urgently required for $X(1870)$ and $\eta_2(1870)$. Some valuable suggestions for the experiments in future are also needed.

The paper is organized as follows. In Section 2, the masses of $X(1870)$ and $\eta_2(1870)$ will be explored in the GI relativized quark model and the Regge trajectories (RTs) framework. In Section 3, the decay processes that an isoscalar meson decays into light scalar (below 1 GeV) and pseudoscalar mesons will be discussed. The two-body strong decays of $X(1870)$ and $\eta_2(1870)$ will be calculated within the $^3P_0$ model and the flux-tube model. Finally, our discussions and conclusions will be presented in Section 4.

2. Mass Spectrum

In the Godfrey-Isgur relativized potential model [20], the Hamiltonian H consists of a central potential and the kinetic term in a "relativized" form

$$H = \sqrt{\vec{p}_q^2 + m_q^2} + \sqrt{\vec{p}_{\bar{q}}^2 + m_{\bar{q}}^2} + V_{q\bar{q}}(r). \quad (3)$$

The funnel-shaped potentials which include a color coulomb term at short distances and a linear scalar confining term at large distances are usually incorporated as the zeroth-order potential. The typical funnel-shaped potential was proposed by the Cornell group (Cornell potential) with the form [29]

$$V_{q\bar{q}}(r) = -\frac{4}{3}\frac{\alpha_s}{r} + \sigma r + C. \quad (4)$$

The strong coupling constant α_s, the string tension σ, and the constant C are the model parameters which can be fixed by the well-established experimental states. The remaining spin-dependent terms for mass shifts are usually treated as the leading-order perturbations which include the spin-spin contact hyperfine interaction, spin-orbit and tensor interactions, and a longer-ranged inverted spin-orbit term. They arise from one gluon exchange (OGE) forces and the assumed Lorentz scalar confinement. The expressions for these terms may be found in [20].

It should be pointed out that the nonperturbative contribution may dominate for the hyperfine splitting of light mesons, which is not like the heavy quarkonium [30]. For example, the hyperfine shift of the $h_c(1P)$ meson with respect to the center gravity of the $\chi_c(1P)$ mesons is much small: $M_{\text{cog}}(\chi_c) - M(h_c) = -0.02 \pm 0.19 \pm 0.13$ MeV [31]. However, for the light isovector mesons $a_0(1450)$, $a_1(1260)$, $a_2(1320)$, and $b_1(1235)$, the hyperfine shift is 76.7 ± 44.4 MeV. Here the masses of a_0, a_1, a_2, and b_1 are taken from PDG [2]. For the complexities of nonperturbative interactions, we are not going to calculate the hyperfine splitting.

Now, the spin-averaged mass, $\overline{M}_{nl}$, of nL multiplet can be obtained by solving the spinless Salpeter equation:

$$\left[\sqrt{\vec{p}_q^2 + m_q^2} + \sqrt{\vec{p}_{\bar{q}}^2 + m_{\bar{q}}^2} + V_{q\bar{q}}(r)\right]\psi(r) = E\psi(r). \quad (5)$$

Here we employ a variational approach described in [32] to solve (5). This variational approach has been applied well in solving the Salpeter equation for $c\bar{s}$ [33], $c\bar{c}$ and $b\bar{b}$ [34] mass spectrum.

In the calculations, the basic simple harmonic oscillator (SHO) functions are taken as the trial wave functions. It is given by

$$\psi_{nl}(r,\beta) = \beta^{3/2}\sqrt{\frac{2(2n-1)!}{\Gamma(n+l+(1/2))}}(\beta r)^l e^{-\beta^2 r^2/2} L_{n-1}^{l+1/2}(\beta^2 r^2) \quad (6)$$

in the position space. Here the SHO function scale β is the variational parameter.

By the Fourier transform, the SHO radial wave function in the momentum is

$$\psi_{nl}(p,\beta) = \frac{(-1)^n}{\beta^{3/2}}\sqrt{\frac{2(2n-1)!}{\Gamma(n+l+(1/2))}}\left(\frac{p}{\beta}\right)^l e^{-p^2/2\beta^2} L_{n-1}^{l+1/2}\left(\frac{p^2}{\beta^2}\right). \quad (7)$$

The wave functions of $\psi_{nl}(r,\beta)$ and $\psi_{nl}(p,\beta)$ meet the normalization conditions:

$$\int_0^\infty \psi_{nl}^2(r,\beta)\, r^2 dr = 1, \qquad \int_0^\infty \psi_{nl}^2(p,\beta)\, p^2 dp = 1. \quad (8)$$

In the variational approach, the corresponding $\overline{M}_{nl}$ are given by minimizing the expectation value of H

$$\frac{d}{d\beta}E_{nl}(\beta) = 0, \quad (9)$$

where

$$E_{nl}(\beta) \equiv \langle H\rangle_{nl} = \langle \psi_{nl}|H|\psi_{nl}\rangle. \quad (10)$$

When all the parameters of the potential model are known, the values of the harmonic oscillator parameter $\overline{\beta}$ can be fixed directly. With the values of $\overline{\beta}$, all the spin-averaged masses $\overline{M}_{nl}$ will be obtained easily. $\overline{M}_{nl}$ obtained in this way trend to be better for the higher-excited states [35].

It is unreasonable to treat the spin-spin contact hyperfine interaction as a perturbation for the ground states, because the mass splitting between pseudoscalar mesons and vector mesons are much large. Then we consider the contributions of $V_{\vec{s}\cdot\vec{s}}(r)$ for the 1S mesons. The following Gaussian-smeared contact hyperfine interaction [36] is taken for convenience:

$$V_{q\bar{q}}^{\vec{s}\cdot\vec{s}}(r) = \frac{32\pi\alpha_s}{9m_q^2}\left(\frac{\kappa}{\sqrt{\pi}}\right)^3 e^{-\kappa^2 r^2}\vec{S}_q\cdot\vec{S}_{\bar{q}}. \quad (11)$$

In this work, we choose the model parameters as follows: $m_u = m_d = 0.220$ GeV, $m_s = 0.428$ GeV, $\alpha_s = 0.6$, $\sigma = 0.143\,\text{GeV}^2$, $\kappa = 0.37$ GeV, and $C = -0.37$ GeV. We take the smaller value of σ here rather than the value in [20]. The smaller σ was obtained by the relation between the slope of the Regge trajectory for the Salpeter equation α' and the slope α'_{st} in the string picture [30]. The Gaussian smearing parameter κ seems a little smaller than that in [20]. However, the κ is usually fitted by the hyperfine splitting of low-excited nS states in the works of literature with a certain arbitrariness.

The values of $\overline{M}_{nL}$ and $\overline{\beta}$ for the states 2S, 3S, 4S, 1P, 2P, 3P, 1D, 2D, 3D, 1F, 2F, 1G, and 1H are listed in Table 1. The experimental masses for the relative mesons are taken from PDG [2].

Obviously, the spin-averaged masses of the 2S, 1P, 1$Dn\bar{n}$ and 1P, and 2$Ss\bar{s}$ mesons are consistent with the experimental data. Indeed, the predicted masses of higher excited states here are also reasonable, for example, $a_4(2040)$ and $f_4(2050)$ are very possible the F-wave $n\bar{n}$ isovector and isoscalar mesons with the masses of 1996^{+10}_{-9} MeV and 2018 ± 11 MeV, respectively [2]. The predicted spin-averaged mass of 1F is not incompatible with experiments. Our results are also overall in good agreement with the expectations from [37]. The trend that a higher excited state corresponds to a smaller $\overline{\beta}$ coincides with [38–40]. For considering the spin-spin contact hyperfine interaction, there are two $\overline{\beta}$s for the 1S mesons. The larger one corresponds to the 1^1S_0 state and the smaller one the 1^3S_1 state.

Table 1: The spin-averaged mass (unit: GeV) and the harmonic oscillator parameter $\overline{\beta}$ (unit: GeV^{-1}) of the states 2S, 3S, 4S, 1P, 2P, 3P, 1D, 2D, 3D, 1F, 2F, 1G, and 1H.

States	$\overline{M}_{nl}(n\bar{n})$	$\overline{\beta}$	Expt. [2]	$\overline{M}_{nl}(s\bar{s})$	$\overline{\beta}$	Expt. [2]
1S	—	0.44/0.34	—	—	0.42/0.39	—
2S	1.399	0.310	1.389	1.631	0.330	1.629
3S	1.859	0.295		**2.069**	0.310	
4S	2.240	0.290		2.436	0.300	
1P	1.252	0.310	1.257	1.460	0.340	1.478
2P	1.711	0.294		**1.926**	0.315	
3P	2.110	0.290		2.308	0.300	
1D	1.661	0.280	1.672	**1.883**	0.300	
2D	**2.067**	0.276		2.272	0.292	
3D	2.417	0.275		2.609	0.288	
1F	1.924	0.277		2.128	0.295	
2F	2.287	0.275		2.478	0.290	
1G	2.161	0.275		2.350	0.292	
1H	2.377	0.273		2.554	0.287	

As shown in [37, 41], the confinement potential $V_{\text{conf}}(r)$ is determinant for the properties of higher excited states. In [37], the masses for higher excited states with $\sigma = 0.143\,\text{GeV}^2$ and $\alpha_s = 0$ are closer to experimental data than the results given in [20]. Then we ignored the Coulomb interaction for 1D, 2D, 1F, 1G, and 1H states. In this way, $\overline{M}_{nl}$ for these states increase about 100 MeV.

The masses of $\eta'(3^1S_0)$, $f_1'(2^3P_1)$, $\eta_2'(1^1D_2)$, and $\eta_2(2^1D_2)$ are usually within 1.8~2.1 GeV in various quark potential models [20, 25–27] (see in Table 2). The predicted spin-averaged masses of 3$S(s\bar{s})$, 2$P(s\bar{s})$, 1$D(s\bar{s})$, and 2$D(n\bar{n})$ are also within this mass regions (bold ones in Table 1). Due to the uncertainty of the potential models, absolute deviation from experimental data are usually about 100~150 MeV for the higher excited states. Compared with these predicted masses, $X(1870)$ disfavors the $\eta'(3^1S_0)$ assignment for its low mass. But the possibilities of $f_1'(2^3P_1)$, $\eta_2'(1^1D_2)$, and $\eta_2(2^1D_2)$ still exist. Here we do not consider the possibility of $X(1870)$ as the $\eta(3^1S_0)$ state because $\eta(1760)$ looks more like a good $\eta(3^1S_0)$ candidate [42–44].

Regge trajectories (RTs) are another useful tool for studying the mass spectrum of the light flavor mesons. In [45], the

Table 2: The masses predicted for $3^1S_0(\eta')$, $2^3P_1(\eta')$, $1^1D_2(\eta')$, and $2^1D_2(\eta)$ in [20, 25–27]. The value denoted by "†" was predicted for the mass of isovector 2^1D_2 state in [20].

States	$\eta'(3^1S_0)$	$f_1'(2^3P_1)$	$\eta_2'(1^1D_2)$	$\eta_2(2^1D_2)$
[20]	—	2030	1890	$2130^\dagger$
[25]	2085	2016	1909	1960
[26]	2099	1988	1851	—
[27]	—	—	1853	1863

Table 3: $X(1870)$ calculated in RTs for different states. The masses of $\eta'(1475)$, $f_1(1420)$, $h_1(1380)$, and $\eta_2(1645)$ are taken from PDG [2].

Four possible states for $X(1870)$			
$\eta'(3^1S_0)$	$f_1'(2^3P_1)$	$\eta_2'(1^1D_2)$	$\eta_2(2^1D_2)$
$\eta'(1475)$	$f_1(1420)$	$h_1(1380)$	$\eta_2(1645)$
$\mu^2 = 1.34^{+0.04}_{-0.03}$	$\mu^2 = 1.38^{+0.04}_{-0.03}$	$\beta^2 = 1.60^{+0.06}_{-0.06}$	$\mu^2 = 0.91^{+0.04}_{-0.03}$

authors fitted the RTs for all light-quark meson states listed in the PDG tables. A global description was constructed as

$$M^2 = 1.38\,(4)\,n + 1.12\,(4)\,J - 1.25\,(4)\,. \tag{12}$$

Here, n and J mean the the radial and angular-momentum quantum number. Recently, the authors of [45] repeated their fits with the subset mesons of the paper [46]. They found a little smaller averaged slopes of $\mu^2 = 1.28(5)\,\mathrm{GeV}^2$ and $\beta^2 = 1.09(6)\,\mathrm{GeV}^2$ to be compared with $\mu^2 = 1.38(4)\,\mathrm{GeV}^2$ and $\beta^2 = 1.12(4)\,\mathrm{GeV}^2$ in (12). Here the μ^2 and β^2 are the weighed averaged slopes for radial and angular-momentum RTs [45, 47].

Now $h_1(1380)$, $f_1(1420)$, and $\eta'(1475)$ have been established as the 1^1P_1, 1^3P_1, and $2^1S_0 s\bar{s}$ states in PDG [2]. With the differences between the mass squared of $X(1870)$ and these states (Table 3), $X(1870)$ could be assigned for the $\eta'(3^1S_0)$ and $f_1'(2^1P_1)$. The mass of $X(1870)$ is too large for the $\eta_2'(1^1D_2)$ state in the RTs. $\eta_2(1645)$ has been assigned as the $1^1D_2 n\bar{n}$ meson [2]. Since $M^2(X(1870)) - M^2(\eta_2(1640)) = 0.91^{+0.04}_{-0.03}\,\mathrm{GeV}^2$ which is much smaller than $1.38(4)\,\mathrm{GeV}^2$, $X(1870)$ looks unlike the $2^1D_2 n\bar{n}$ state for its low mass. However, the difference of $M^2(X(1870)) - M^2(h_1(1170)) = 2.16^{+0.06}_{-0.05}\,\mathrm{GeV}^2$ matches the slopes $2.37(11)\,\mathrm{GeV}^2$ well. Then the RTs can not exclude the possibility of $X(1870)$ as the $2^1D_2 n\bar{n}$ state.

As mentioned in Section 1, $X(1870)$ is also a good hybrid candidate since its mass overlaps the predictions given by different models. The predicted masses for 0^+0^{-+}, 0^+1^{++}, and 0^+2^{-+} $n\bar{n}g$ states by these models are collected in Table 4.

In this section, the mass of $X(1870)$ has been studied in the GI quark potential model and the RTs framework. In the GI quark potential model, $X(1870)$ can be interpreted as the $f_1'(2^3P_1)$, $\eta_2'(1^1D_2)$, or $\eta_2(2^1D_2)$ state with a reasonable uncertainty. In the RTs, $X(1870)$ favors the $\eta'(3^1S_0)$ and $f_1'(2^3P_1)$ assignments. But the $\eta_2(2^1D_2)$ assignment can not be excluded thoroughly. $X(1870)$ is also a good hybrid state candidate. Since the masses of $X(1870)$ and $\eta_2(1870)$ are nearly equal, the possible assignments of $X(1870)$ also suit $\eta_2(1870)$. The investigations of the strong decay properties will be more helpful to distinguish the $\eta_2(1870)$ and $X(1870)$.

Table 4: The masses predicted for $\eta_H(0^+0^{-+})$, $f_H(0^+1^{++})$ and $\eta_H(0^+2^{-+})$ hybrid states in [11–15].

States	$\eta_H(0^+0^{-+})$	$f_H(0^+1^{++})$	$\eta_H(0^+2^{-+})$
Bag [11, 12]	1.3	Heavier	1.9
Flux tube [13, 14]	1.7~1.9	1.7~1.9	1.7~1.9
Constituent gluon [15]	1.8~2.2	1.3~1.8	1.8~2.2

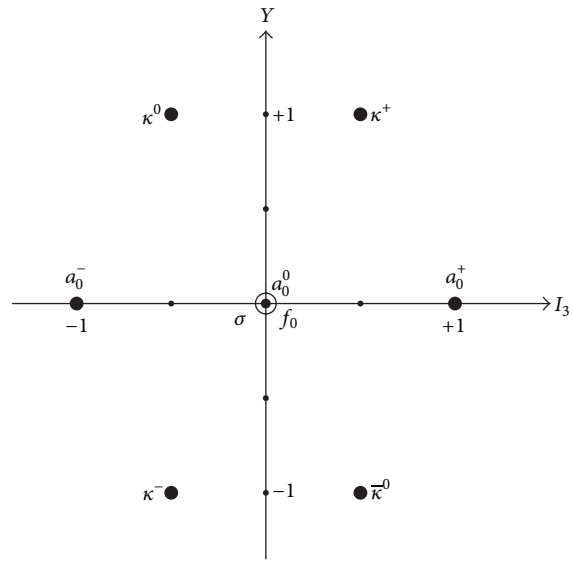

Figure 2: The "$\mathcal{S}$" nonet below 1 GeV shown in Y-I_3 plane.

3. The Strong Decay

3.1. The Final Mesons Include the Scalar Mesons below 1 GeV. Despite many theoretical efforts, the scalar nonet of $q\bar{q}$ mesons has never established well. The lowest-lying scalar mesons including $\sigma(500)$ (or $f_0(600)$), $\kappa(800)$, $a_0(980)$, and $f_0(980)$ are difficult to be described as $q\bar{q}$ states; for example, $a_0(980)$ is associated with nonstrange quarks in the $q\bar{q}$ scheme. If this is true, its high mass and decay properties are difficult to be understood simultaneously. So interpretations as exotic states were triggered, For examples, two clusters of two quarks and two antiquarks [48], particular quasi-molecular states [49–51], and uncorrelated four-quark states $qq\bar{q}\bar{q}$ [52–54] have been proposed.

Though the structures of these scalar mesons below 1 GeV are still in dispute, the viewpoint that these scalar mesons can constitute a complete nonet states has been reached in most works of the literature (as illustrated in Figure 2). In the following, we will denote this nonet as "$\mathcal{S}$" multiplet for convenience.

Due to the unclear nature of the $\mathcal{S}$ mesons, it seems much difficult to study the decay processes when the final mesons include a $\mathcal{S}$ member. As an approximation, $a_0(980)$, $\sigma(500)$, and $f_0(980)$ were treated as 1^3P_0 $q\bar{q}$ mesons in [44, 55]. In

[24, 43], this kind of decay channel was ignored. However, this kind of decay mode may be predominant for some mesons. For example, the observations indicate that $f_1(1285)$, $\eta(1405)$, and $X(1870)$ primarily decay via the $a_0(980)\pi$ channel [1].

In what follows, we will extract some useful information about this kind of decay mode by the SU(3) flavor symmetry. We will show that $a_0(980)\pi$, $\sigma_0\eta$, and $f_0\eta$ are the main decay channels for the isoscalar $n\bar{n}$ and the $n\bar{n}g$ mesons when they decay primarily through "$\mathcal{S}+P$" mesons, where the sign "P" denotes a light pseudoscalar meson. This will explain why $X(1870)$ has been first observed in the $\eta\pi^+\pi^-$ channel.

We noticed that the $\mathcal{S}$ nonet could be interpreted like the $q\bar{q}$ nonet in the diquark-antidiquark scenario. In Wilczek and Jaffe's terminology [56, 57], the $\mathcal{S}$ mesons consist of a "good" diquark and a "good" antidiquark. When u, d quarks form a "good" diquark, it means that the two light quarks, u and d, could be treated as a quasiparticle in color $\bar{3}$, flavor $\bar{3}$, and the spin singlet. The "good" u, d diquark is usually denoted as $[ud]$.

In the diquark-antidiquark limit, the parity of a tetraquark is determined by $P=(-1)^{L_{12-34}}$ [58] where the L_{12-34} refers to the relative angular momentum between two clusters. Thus the $\mathcal{S}$ mesons are the lightest tetraquark states in the diquark-antidiquark model with $L_{12-34}=0$. The $\mathcal{S}$ nonet in the full set of flavor representations is

$$(3\otimes 3)_{\bar{3}}\otimes\left(\bar{3}\otimes\bar{3}\right)_3=8\oplus 1. \tag{13}$$

Because the SU(3) flavor symmetry is not exact, the two physical isoscalar mesons, σ_0 and f_0, are usually the mixing states of the $|8\rangle_{I=0}$ and $|1\rangle_{I=0}$ states [48],

$$\begin{pmatrix} f_0 \\ \sigma_0 \end{pmatrix}=\begin{pmatrix} \cos\vartheta & \sin\vartheta \\ -\sin\vartheta & \cos\vartheta \end{pmatrix}\begin{pmatrix} |8\rangle_{I=0} \\ |1\rangle_{I=0} \end{pmatrix}. \tag{14}$$

When the mixing angle ϑ equals the so-called ideal mixing angle, that is, $\vartheta=54.74^\circ$, the composition of the $\sigma(500)$ and $f_0(980)$ is

$$\begin{pmatrix} f_0 \\ \sigma_0 \end{pmatrix}=\begin{pmatrix} \left|\frac{1}{\sqrt{2}}\left([su]\,[\bar{s}\,\bar{u}]+[sd]\left[\bar{s}\bar{d}\right]\right)\right\rangle \\ \left|[ud]\left[\bar{u}\bar{d}\right]\right\rangle \end{pmatrix}. \tag{15}$$

It seems that the deviation from the ideal mixing angle of the $\sigma(500)$ and $f_0(980)$ is small [48]. In the following calculations, we will treat them in the ideal mixing scheme.

Under the SU(3) flavor assumption, all the members of the octet have the same basic coupling constant in one type of reaction, while the singlet member has a different coupling constant. Particularly, when a quarkonium decays into $\mathcal{S}$ and $q\bar{q}$ mesons, there are five independent coupling constants, that is, g_{A88}, g_{A81}, g_{A18}, g_{B88}, and g_{B11}, corresponding to five different channels

$$\begin{aligned}
|8\rangle_{q\bar{q}} &\longrightarrow |8\rangle_{\mathcal{S}}\otimes|8\rangle_{q\bar{q}}: \quad g_{A88}, \\
|8\rangle_{q\bar{q}} &\longrightarrow |8\rangle_{\mathcal{S}}\otimes|1\rangle_{q\bar{q}}: \quad g_{A81}, \\
|8\rangle_{q\bar{q}} &\longrightarrow |1\rangle_{\mathcal{S}}\otimes|8\rangle_{q\bar{q}}: \quad g_{A18}, \\
|1\rangle_{q\bar{q}} &\longrightarrow |8\rangle_{\mathcal{S}}\otimes|8\rangle_{q\bar{q}}: \quad g_{B88}, \\
|1\rangle_{q\bar{q}} &\longrightarrow |1\rangle_{\mathcal{S}}\otimes|1\rangle_{q\bar{q}}: \quad g_{B11}.
\end{aligned} \tag{16}$$

In order to determine the relations between these coupling constants, we will assume the process that the $q\bar{q}$ or $q\bar{q}g$ meson decays into a $\mathcal{S}$ and another $q\bar{q}$ mesons obey the OZI (Okubo-Zweig-Iizuka) rule; that is, the two quarks in the mother meson go into two daughter mesons, respectively. Therefore, there are four forbidden processes: $X((1/\sqrt{2})(u\bar{u}-d\bar{d}))\nrightarrow a_0+s\bar{s}$, $X((1/\sqrt{2})(u\bar{u}+d\bar{d}))\nrightarrow\sigma_0+s\bar{s}$, $X(s\bar{s})\nrightarrow f_0+(1/\sqrt{2})(u\bar{u}+d\bar{d})$ and $X(s\bar{s})\nrightarrow\sigma_0+s\bar{s}$. With the help of the SU(3) Clebsch-Gordan coefficients [59], the ratios between the five coupling constants are extracted as

$$\begin{aligned}
&g_{A81}:g_{A18}:g_{B88}:g_{B11}:g_{A88} \\
&\quad=\sqrt{2}:-\sqrt{\frac{2}{5}}\left(\sqrt{5}+1\right):-\frac{2}{\sqrt{5}}\left(\sqrt{5}+1\right): \\
&\qquad-\sqrt{\frac{2}{5}}\left(\sqrt{5}+1\right):1 \\
&\quad\approx 1.41:-2.05:-2.89:-2.05:1.00.
\end{aligned} \tag{17}$$

It is well known that the physical states, $\eta(548)$ and $\eta'(958)$, are the mixture of the SU(3) flavor octet and singlet. They can be written in terms of a mixing angle, θ_p, as follows:

$$\begin{pmatrix} \eta(548) \\ \eta'(958) \end{pmatrix}=\begin{pmatrix} \cos\theta_p & -\sin\theta_p \\ \sin\theta_p & \cos\theta_p \end{pmatrix}\begin{pmatrix} |8\rangle_{I=0} \\ |1\rangle_{I=0} \end{pmatrix}. \tag{18}$$

The mixing angle θ_p has been measured by various means. However, there is still uncertainty for θ_p. An excellent fit to the tensor meson decay widths was performed under the SU(3) symmetry, and $\theta_p\simeq-17^\circ$ was obtained [23]. In our calculation, θ_p is taken as -17°. The excited mixtures of $n\bar{n}$ and $s\bar{s}$ are denoted as

$$\begin{pmatrix} \xi \\ \xi' \end{pmatrix}=\begin{pmatrix} \cos\theta & \sin\theta \\ -\sin\theta & \cos\theta \end{pmatrix}\begin{pmatrix} |1\rangle_{I=0} \\ |8\rangle_{I=0} \end{pmatrix}. \tag{19}$$

In this scheme, the ideal mixing occurs with the choice of $\theta=35.3^\circ$. When ξ and ξ' decay into a $\mathcal{S}$ and pseudoscalar mesons, the relations of decay amplitudes are governed by the coefficients ζ^2 which are model-independent in the limitation of $\mathrm{SU}(3)_f$ symmetry. With the coupling constants in hand, the coefficients ζ^2 of ξ and ξ' versus the mixing angle θ are shown in the Figures 3 and 4. When ξ and ξ' occur in the ideal mixing, the values of ζ^2 are presented in Table 5. In the factorization framework, the decay difference of a hybrid and excited $q\bar{q}$ mesons comes from the spatial contraction [60]. Then the coefficients ζ^2 for hybrid states are the same as these of $q\bar{q}$ quarkonia.

Here the mixing of $\eta(548)$ and $\eta'(958)$ has been considered. It is sure that the ζ^2 are zero for the processes $\xi'\to a_0\pi$, $\xi'\to\sigma\eta$, and $\xi'\to\sigma\eta'$, since they are OZI-forbidden. ζ^2 of $\xi'\to f_0\eta'$ has not been considered in Table 5 since $X(1870)$ lies below the threshold of $f_0\eta'$.

As illustrated in Figures 3 and 4, the primary decay channels of a $s\bar{s}$ or $s\bar{s}g$ predominant excitation are $f_0\eta$ and κK. If the deviation of θ from the ideal mixing angle is not large, $X(1870)$ should be a $n\bar{n}$ or $n\bar{n}g$ predominant state

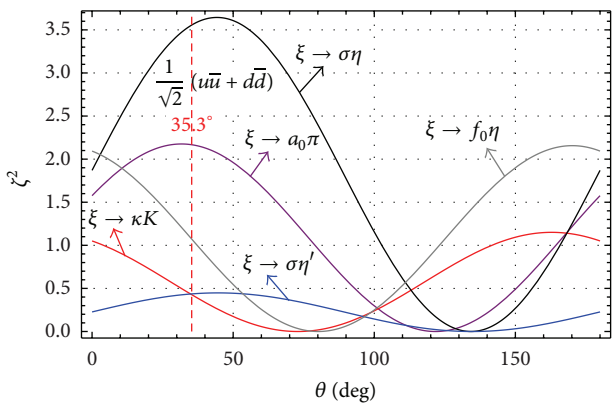

Figure 3: The coefficients ζ^2 of the isoscalar meson ξ versus the mixing angle θ.

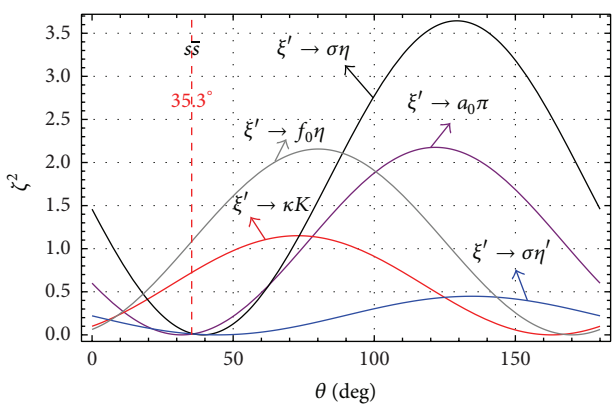

Figure 4: The coefficients ζ^2 of the isoscalar meson ξ' versus the mixing angle θ.

Table 5: The coefficients ζ^2 of ξ and ξ' in the ideal mixing.

Decay channels	$a_0\pi$	$\sigma\eta$	κK	$f_0\eta$	$\sigma\eta'$
$\zeta^2\,[n\bar{n}(g)]$	2.17	3.56	0.47	1.07	0.44
$\zeta^2\,[s\bar{s}(g)]$	0.00	0.00	0.72	1.08	0.00

since $X(1870)$ primarily decays via the $a_0(980)\pi$ channel. At present, only the ground 0^{-+} and the 0^{++} isoscalar mesons deviate from the ideal mixing distinctly. In addition, if the $X(1870)$ is produced via a diagram of Figure 1(b), it should also be $n\bar{n}$ or $n\bar{n}g$ predominant state.

Of course, the $SU(3)_f$ symmetry breaking will affect the ratios of these channels listed in Table 5, because the three-momentum of the these products are different. However, the coefficients ζ^2 have presented the valuable information for these specific decay channels. When $\eta_2(1870)$ occupies the $2^1D_2 n\bar{n}$ state, $X(1870)$ becomes a good $n\bar{n}g$ candidate. In the following subsection, we will explore the two-body strong decays of $X(1870)$ within the $^3P_0$ model and the flux-tube model. Of course, the analysis of $X(1870)$ also suits $\eta_2(1870)$ for their nearly equal masses.

3.2. The Strong Decays of $\eta_2(1870)$ and $X(1870)$. In [24], the $^3P_0$ model [61–63] and the flux-tube model [64] were employed to study the two-body strong decays of $\eta_2(1870)$. There, the pair production (creation) strength γ and the simple harmonic oscillator (SHO) wave function scale parameter, βs, were taken as constants.

However, a series of studies indicate that the strength γ may depend on both the flavor and the relative momentum of the produced quarks [28, 65]. γ may also depend on the reduced mass of quark-antiquark pair of the decaying meson [66]. Firstly, the relations of the $^3P_0$ model to "microscopic" QCD decay mechanisms have been studied in [65]. There, the authors found that the constant γ corresponds approximately to the dimensionless combination, $\sigma/m_q\beta$, where m_q is the mass of produced quark, β means the meson wave function scale, and σ is the string tension. Secondly, the momentum dependent manner of γ has been studied in [28]. It was found that γ is dependent on the relative momentum of the created $q\bar{q}$ pair, and the form of $\gamma(k) = A + B\exp(-Ck^2)$ with $k = |\vec{k}_3 - \vec{k}_4|$ was suggested. Thirdly, Segovia et al. proposed that γ is a function of the reduced mass of quark-antiquark pair of the decaying meson [66]. Based on the first and third points above, γ will depend on the flavors of both the decaying meson and produced pairs. In our calculations, we will treat the γ as a free parameter and fix it by the well-measured partial decay widths.

In addition, the amplitudes given by the $^3P_0$ model and the flux-tube model often contain the nodal-type Gaussian form factors which can lead to a dynamic suppression for some channels. Then the values of β are important to extract the decay width for the higher excited mesons in these two strong decay models.

In the following, the two-body strong decay of $X(1870)$ will be investigated in the $^3P_0$ model where the strength γ will be extracted by fitting the experimental data. The SHO wave function scale parameter, βs, will be borrowed from Table 1 which are extracted by the GI relativized potential model. We will also check the possibility of $X(1870)$ as a possible hybrid state by the flux-tube model.

In the nonrelativistic limit, the transition operator $\widehat{\mathcal{T}}$ of the $^3P_0$ model is depicted as

$$\begin{aligned}\widehat{\mathcal{T}} = &-3\gamma\sum_m \langle 1, m; 1, -m \mid 0, 0\rangle \\ &\times \iint d^3\vec{k}_3 d^3\vec{k}_4 \delta^3\left(\vec{k}_3 + \vec{k}_4\right) \\ &\times \mathcal{Y}_1^m\left(\frac{\vec{k}_3 - \vec{k}_4}{2}\right)\omega_0^{(3,4)}\varphi_0^{(3,4)}\chi_{1,-m}^{(3,4)} d_{3i}^{\dagger}\left(\vec{k}_3\right) d_{4j}^{\dagger}\left(\vec{k}_4\right),\end{aligned} \tag{20}$$

where the $\omega_0^{(3,4)}$ and $\varphi_0^{(3,4)}$ are the color and flavor wave functions of the $q_3\bar{q}_4$ pair created from vacuum. Thus, $\omega_0^{(3,4)} = (R\bar{R} + G\bar{G} + B\bar{B})/\sqrt{3}$, $\varphi_0^{(3,4)} = (u\bar{u} + d\bar{d} + s\bar{s})/\sqrt{3}$ are color and flavor singlets. The pair is also assumed to carry the quantum numbers of 0^{++}, suggesting that they are in a $^3P_0$ state. Then $\chi_{1,-m}^{(3,4)}$ represents the pair production in a spin triplet state.

The solid harmonic polynomial $\mathscr{Y}_1^m(\vec{k}) \equiv |\vec{k}|\mathscr{Y}_1^m(\theta_k, \phi_k)$ reflects the momentum-space distribution of the $q_3\bar{q}_4$.

The helicity amplitude $\mathscr{M}^{M_{J_A}, M_{J_B}, M_{J_C}}(p)$ of $A \to B + C$ is given by

$$\left\langle BC \left| \widehat{\mathscr{T}} \right| A \right\rangle = \delta^3\left(\vec{P}_A - \vec{P}_B - \vec{P}_C\right) \mathscr{M}^{M_{J_A}, M_{J_B}, M_{J_C}}(p), \quad (21)$$

where p represents the momentum of the outgoing meson in the rest frame of the meson A. When the mock state [67] is adopted to describe the spatial wave function of a meson, the helicity amplitude $\mathscr{M}^{M_{J_A}, M_{J_B}, M_{J_C}}(p)$ can be constructed in the $L - S$ basis easily [62, 63]. The mock state for A meson is

$$\begin{aligned} &\left| A\left(n_A{}^{2S_A+1}L_A^{J_A M_{J_A}}\left(\vec{P}_A\right)\right)\right\rangle \\ &\quad \equiv \sqrt{2E_A} \sum_{M_{L_A} M_{S_A}} \left\langle L_A M_{L_A} S_A \mid J_A M_{J_A}\right\rangle \omega_A^{12} \phi_A^{12} \chi_{S_A M_{S_A}}^{12} \\ &\qquad \times \int d\vec{P}_A \psi_{n_A}^{L_A M_{L_A}}\left(\vec{k}_1, \vec{k}_2\right) \left| q_1\left(\vec{k}_1\right) q_2\left(\vec{k}_2\right)\right\rangle. \end{aligned} \quad (22)$$

To obtain the analytical amplitudes, the SHO wave functions are usually employed for $\psi_{n_A}^{L_A M_{L_A}}(\vec{k}_1, \vec{k}_2)$. For comparison with experiments, one obtains the partial decay width $\mathscr{M}^{JL}(p)$ via the Jacob-Wick formula [68]:

$$\begin{aligned} \mathscr{M}_{LS}(p) = &\frac{\sqrt{2L+1}}{2J_A+1} \sum_{M_{J_B}, M_{J_C}} \left\langle L0JM_{J_A} \mid J_A M_{J_A}\right\rangle \\ &\times \left\langle J_B, M_{J_B} J_C, M_{J_C} \mid JM_{J_A}\right\rangle \mathscr{M}^{M_{J_A}, M_{J_B}, M_{J_C}}(p). \end{aligned} \quad (23)$$

Finally, the decay width $\Gamma(A \to BC)$ is derived analytically in terms of the partial wave amplitudes

$$\Gamma(A \longrightarrow BC) = 2\pi \frac{E_B E_C}{M_A} p \sum_{LS} \left|\mathscr{M}_{LS}(p)\right|^2. \quad (24)$$

More technical details of the $^3P_0$ model can be found in [63]. The inherent uncertainties of the $^3P_0$ decay model itself have been discussed in [28, 69, 70].

The dimensionless parameter γ will be fixed by the 8 well-measured partial decay widths which are listed in Table 6. The $\mathscr{M}_{LS}$ amplitudes of these decay channels are presented explicitly in Appendix A.

As mentioned before, γ may depend on the flavors of both the decaying meson and produced pairs. Then we divide the 8 decay channels into two groups: one is $n\bar{n} \to n\bar{n} + n\bar{n}$, and the other includes $s\bar{s} \to n\bar{s} + s\bar{n}$ and $n\bar{n} \to n\bar{s} + s\bar{n}$. The values of γ here are a little different from these given in [28] where an $AL1$ potential (for details of $AL1$ potential, see [35]) was selected to determine the meson wave functions. Of course, the meson wave function given by different potentials will influence the values of γ.

It is clear in Table 6 that γ decrease with p increase. In addition, our calculation indicates that γ depends on flavors of both the decaying meson and the produced quark pairs.

Table 6: Values of γ in different channels and comparison with the results given in [28]. Here, $\rho(770)$, $a_2(1320)$, $f_1'(1420)$, $f_2(1270)$, $f_2'(1525)$ and $\rho_3(1690)$ have been studied.

Decay channels	p (GeV)	γ (10^3)	γ [28]
$\rho \to \pi\pi$	0.362	17.8	9.18
$a_2 \to \eta\pi$	0.535	11.5	—
$f_2 \to \pi\pi$	0.622	7.8	7.13
$\rho_3 \to \pi\pi$	0.833	4.2	—
$f_1' \to K^*\bar{K}$	0.158	4.9	—
$f_2 \to K\bar{K}$	0.401	2.9	6.11
$a_2 \to K\bar{K}$	0.434	2.3	3.91
$f_2' \to K\bar{K}$	0.579	2.0	5.66

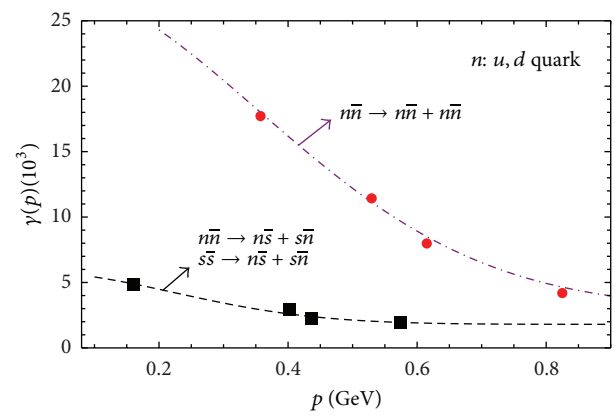

Figure 5: The functions of $\gamma(p) = A + B\exp(-Cp^2)$ in different decay processes. The symbols of red "●" and black "■" denote γ values determined by the experimental data.

For example, values of γ fixed by $a_2 \to K\bar{K}$ and $f_2' \to K\bar{K}$ are roughly equal.

In the following calculations, we assume that the values of γ corresponding to the processes of $s\bar{s} \to n\bar{s} + s\bar{n}$ and $n\bar{n} \to n\bar{s} + s\bar{n}$ are determined by one function. Similarly, we take the function, $\gamma(p) = A + B\exp(-Cp^2)$, for the creation vertex. *The function of the creation vertex here is different from the one used in* [28]. With the four decay channels listed in the fifth column of Table 6, we fix the function as $\gamma(p) = 1.8 + 4\exp(-10p^2)$. For the processes of $n\bar{n} \to n\bar{n} + n\bar{n}$ (the first column of Table 6), we fix the creation vertex function as $\gamma(p) = 3.0 + 25\exp(-4p^2)$. The dependence of γ on the momentum p is plotted in Figure 5. Obviously the functions can describe the dependence of γ and p well. The functions of creation vertex given here need further test.

Since we neglected the mass splitting within the isospin multiplet, the partial width into the specific charge channel should be multiplied by the flavor multiplicity factor $\mathscr{F}$ (Table 7). This $\mathscr{F}$ factor also incorporates the statistical factor 1/2 if the final state mesons B and C are identical (as illustrated in Figure 6). More details of $\mathscr{F}$ can be found in the Appendix A of [71].

The partial decay widths of $X(1870)$ are shown in Table 8 except the channels of $\mathscr{S}+P$ mesons. $a_2(1320)\pi$ and $f_2(1275)\eta$ are large channels for the $\eta_2(2^1D_2)n\bar{n}$ state in our work and

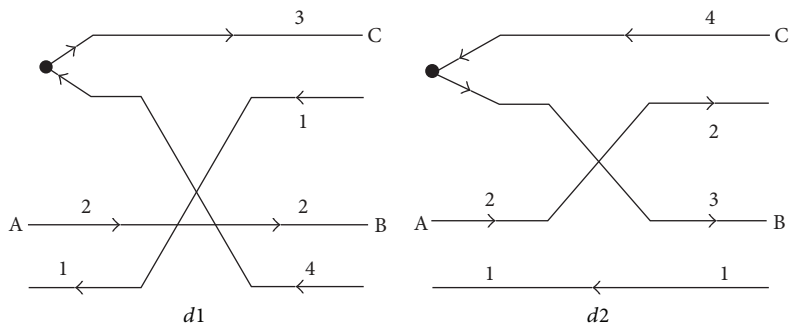

Figure 6: Two topological diagrams for a $q\bar{q}$ meson decay in the $^3P_0$ decay model. We refer to the left one as $d1$ where the produced quark goes into meson C and $d2$ where it goes into B.

Table 7: The second and third columns for the flavor weight factors corresponding to two topological diagrams shown in Figure 6. The last column for the flavor multiplicity factor $\mathcal{F}$. Here, $|\eta\rangle = (|n\bar{n}\rangle - |s\bar{s}\rangle)/\sqrt{2}$ and $|\eta'\rangle = (|n\bar{n}\rangle + |s\bar{s}\rangle)/\sqrt{2}$ have been taken for simplicity.

Decay channels	$\mathcal{I}_{\text{flavor}}(d1)$	$\mathcal{I}_{\text{flavor}}(d1)$	$\mathcal{F}$
$\rho \to \pi\pi$	$+1/\sqrt{2}$	$-1/\sqrt{2}$	1
$f_2 \to \pi\pi$	$-1/\sqrt{2}$	$-1/\sqrt{2}$	3/2
$f_2 \to KK$	0	$-1/\sqrt{2}$	2
$f_1' \to K^*K$	+1	0	4
$f_2' \to KK$	+1	0	2
$a_2 \to KK$	0	−1	1
$a_2 \to \eta\pi$	+1/2	+1/2	1
$\eta_2 \to \omega\omega$	$-1/\sqrt{2}$	$-1/\sqrt{2}$	1/2
$\eta_2 \to a_i\pi$	$-1/\sqrt{2}$	$-1/\sqrt{2}$	3
$\eta_2 \to f_i\eta$	+1/2	+1/2	1

[24], which are consistent with the experimental observations of the $\eta_2(1870)$. The partial widths of K^*K, $\rho\rho$, and $\omega\omega$ are narrower in our work than the expectations from [24]. $\eta_2(1870)$ has been observed by the BES Collaboration in the radiative decay channel of $J/\psi \to \gamma\eta\pi\pi$ [24]. However, no apparent $\eta_2(1870)$ signals were detected in the channels of $J/\psi \to \gamma\rho\rho$ [72] and $J/\psi \to \gamma\omega\omega$ [73, 74]. Therefore, improved experimental measurements of the radiative J/ψ decay channels are needed for the $\eta_2(1870)$ in future.

Next, we will evaluate the partial widths of "$\mathcal{S} + P$" channels which have not been listed in Table 8. *The scheme is proposed as follows.* As illustrated in Figure 7, we assume that $X(1870)$ decays into $a_0(980)\pi$ via a virtual intermediate $1^3P_0q\bar{q}$ meson. We notice that the $\eta(1295)$ also dominantly decays into the $\eta\pi\pi$ [1]. Its three-body decay can occur via three intermediate processes: $\eta(1295) \to \eta\sigma/a_0(980)\pi/\eta(\pi\pi)_{S\text{-wave}} \to \eta\pi\pi$ [2]. With the ratio $\Gamma(a_0(980)\pi)/\Gamma(\eta\pi\pi) = 0.65 \pm 0.10$ and $\Gamma(\eta(1295)) = 55 \pm 5$ MeV, the partial width of $\eta(1295)$ decaying into $a_0(980)\pi$ is estimated no more than 45 MeV. By the $^3P_0$ model, the ratio of $(\Gamma(X(1870) \to a_0(1^3P_0)\pi))/(\Gamma(\eta(1295) \to a_0(1^3P_0)\pi))$ can be reached easily. If the uncertainty of the coupling vertex of $\varepsilon(1^3P_0(q\bar{q}) \to a_0(980))$ (see in Figure 7) is assumed to

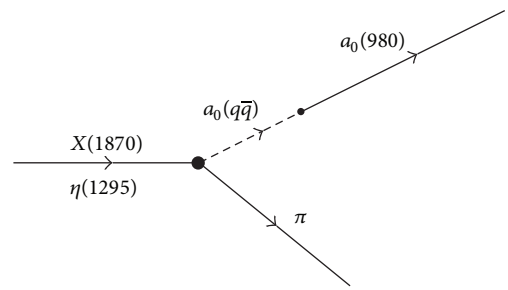

Figure 7: The diagram for the "$\mathcal{S} + P$" channels through a virtual intermediate $1^3P_0q\bar{q}$ meson.

be canceled in the ratio of $(\Gamma(X(1870) \to a_0(1^3P_0)\pi) \cdot \varepsilon(1^3P_0(q\bar{q}) \to a_0(980)))/(\Gamma(\eta(1295) \to a_0(1^3P_0)\pi) \cdot \varepsilon(1^3P_0(q\bar{q}) \to a_0(980)))$, the value of $(\Gamma(X(1870) \to a_0(980)\pi))/(\Gamma(\eta(1295) \to a_0(980)\pi))$ can be extracted roughly. Although the assumption above seems a little rough, we just need to evaluate magnitudes of these decay channels.

$\eta(1295)$ is proposed to be the first radial excited state of $\eta(550)$. Then the total decay widths of $\Gamma(X(1870) \to \mathcal{S} + P)$ are evaluated no more than 12.6 MeV and $\Gamma(X(1870) \to a_0(980)\pi) \leq 3.8$ MeV. The BESIII Collaboration claimed that $X(1870)$ primarily decay via $a_0(980)\pi$ [1]. The small partial width of $\Gamma(X(1870) \to a_0(980)\pi)$ also indicates that the $X(1870)$ can not be interpreted as the $2^1D_2q\bar{q}$ state.

In addition, our results do not support $X(1870)$ as the $\eta_2(2^1D_2)n\bar{n}$ state since its observed decay width is much smaller than the theoretical estimate. The $a_2(1320)\pi$ is the largest decay channel in our numerical results and in [24] for the $\eta_2(2^1D_2)n\bar{n}$ state (Table 8). If the partial width of $a_0(980)\pi$ channel is as large as $a_2(1320)\pi$, the predicted width of $X(1870)$ will be much larger than the observed value.

We adopt the flux tube model to check the possibility of $X(1870)$ as a hybrid meson. The partial widths are also listed in Table 8 for the comparison. Details of the flux model are collected in Appendix B.

Two groups of the partial widths predicted in [16] are quoted in the Table 8. The left column was given by the flux tube decay model of Isgur, Kokoski, and Paton (IKP) with

Table 8: The partial widths of $X(1870)$ and compared with results from [16, 24].

Decay channels	$\eta_2(2^1D_2)$			$\eta_H(0^+0^{-+})$			$f_H(0^+1^{++})$			$\eta_H(0^+2^{-+})$		
	Our	[24]		Our	[16]		Our	[16]		Our	[16]	
K^*K	0.5	17.7	19.3	12.6	10	5	4.9	24.1	18.0	3.2	2.0	1.0
$\rho\rho$	12.9	52.2	56.8	×	×	×	×	×	×	×	×	×
$\omega\omega$	4.2	16.9	18.4	×	×	×	×	×	×	×	×	×
K^*K^*	0.2	2.1	2.3	×	×	×	×	×	×	×	×	×
$a_0(1450)\pi$	16.0	2.4	2.6	56.3	70	175	0.5	×	6	0.5	0.0	0.6
$a_1(1260)\pi$	0.0	15.2	16.6	×	×	×	57.3	14	232	×	0.3	×
$f_1(1280)\eta$	0.0	0.0	0.0	×	×	×	2.5	—	—	×	0.0	×
$a_2(1320)\pi$	54.2	102.5	111.6	8.8	1	16	35.1	5.0	179.4	26.7	25.1	67
$f_2(1275)\eta$	15.1	17.5	19.0	0.0	×	×	1.0	—	—	4.6	0.0	0.0
$\sum\Gamma_i$	103.3	26.5	246.7	77.7	81	196	101.3	43.1	435.4	35.0	27.4	68.6
Expt (MeV)		225 ± 14 [2]						$57 \pm 12^{+19}_{-4}$ [1]				

The symbol "×" indicates that the decay modes are forbidden and "—" denotes that the decay channels can be ignored. Here, we collected the results given by the $^3P_0$ model from [24] in the left column and the right column by the flux-tube model. In [16], the masses are taken as 1.8 GeV for the 0^{-+}, 1^{++}, and 2^{-+} hybrid states.

the "standard parameters" [75]. The right column was by the developed flux tube decay model of Swanson-Szczepaniak (SS). In [16], the masses are taken as 1.8 GeV for the 0^{-+}, 1^{++}, and 2^{-+} hybrid states.

For a hybrid meson, $X(1870)$ seems most possible to be the $\eta_H(0^+2^{-+})$ state because the total widths which exclude the channels of $\mathcal{S}+P$ are much narrow in our work and in [16]. It is consistent with the narrow width of $X(1870)$.

As shown in Table 8, $X(1870)$ is impossible to be the $\eta_H(0^+0^{-+})$ hybrid state. The predicted width in both our work and in [16] is broader. In addition, $\eta\pi$ is a visible channel for both $a_0(1450)$. A week signal was found in the region of 1200~1400 MeV in the analysis of $\eta\pi^{\pm}$ (Figure 2(b) of [1]), which contradicts the large $a_0(1450)\pi$ channel of the $\eta_H(0^+0^{-+})$ state. We can exclude the possibility of $X(1870)$ as the $\eta_H(0^+0^{-+})$ hybrid state preliminarily.

The assignment for $X(1870)$ as the $f_H(0^+1^{++})$ hybrid seems impossible since the theoretical width of $a_1(1260)\pi$ is rather broad in our results and in the IKP model. If the partial width of $a_0(980)\pi$ channel is as large as $a_1(1260)\pi$, the total widths of $X(1870)$ will be much broader than the experimental value. But the width given by the SS flux tube decay model for the $f_H(0^+1^{++})$ hybrid is much small. So the possibility of $X(1870)$ as a $f_H(0^+1^{++})$ hybrid cannot be excluded. We suggest to detect the decay channel of $a_1(1260)\pi$ because this channel is forbidden for the $\eta_H(0^+2^{-+})$ state in the IKP flux tube decay model and very small in the SS flux tube decay model (see Table 8). Then the channel of $a_1(1260)\pi$ can discriminate the states $f_H(0^+1^{++})$ and $\eta_H(0^+2^{-+})$ for $X(1870)$.

Finally, if $\eta_2(1870)$ is the $\eta_2(2^1D_2)$ state, its decay width is predicted about 100 MeV which is much smaller than the experiments. However, the difference can be explained by the remedy of mixing effect. If $X(1870)$ and $\eta_2(1870)$ have the same quantum numbers, 0^+2^{-+}, they should mix with each other with a visible mixing angle. Then the interference enhancement will enlarge the width of $\eta_2(1870)$. The broad decay width of $\eta_2(1870)$ could be explained naturally. On the other hand, $\eta_2(1870)$ has been observed in the channel of $a_0(980)\pi$. However, this channel seems much small if $\eta_2(1870)$ is a pure $2^1D_2 n\bar{n}$ meson. The mixing effect will also enlarge this partial width. Here, we do not plan to discuss the mixing of $X(1870)$ and $\eta_2(1870)$ further for the complex mechanism.

4. Discussions and Conclusions

A isoscalar resonant structure of $X(1870)$ was observed by BESIII in the channels $J/\psi \to \omega X(1870) \to \omega\eta\pi^+\pi^-$ recently. Although the mass of $X(1870)$ is consistent with the $\eta_2(1870)$, the production, decay width, and decay properties are much different. In this paper, the mass spectrum and strong decays of the $X(1870)$ and $\eta_2(1870)$ are analyzed.

Firstly, the mass spectrum is studied in the GI potential model and the RTs framework. In the GI potential model, both $X(1870)$ and $\eta_2(1870)$ could be the $\eta_2'(1^1D_2)$, $f_1'(2^3P_1)$, and $\eta_2(2^1D_2)$ states. In RTs, the possible assignments are the $\eta(3^1S_0)$, $f_1'(2^3P_1)$ and $\eta_2(2^1D_2)$ states. For the mass spectrum, they are also good hybrid candidates since the masses overlap the predictions given by different models (see Table 4).

Secondly, the processes of a $n\bar{n}$ quarkonium or a $n\bar{n}g$ hybrid meson decaying into the "$\mathcal{S}+P$" mesons are studied under the $SU(3)_f$ symmetry and the diquark-antidiquark description of the $\mathcal{S}$ mesons. We assumed that the processes obey the OZI rule. We find that the channels of $a_0\pi$, $\sigma\eta$, and $f_0\eta$ are the dominant when a $n\bar{n}$ quarkonium or a $n\bar{n}g$ hybrid meson decays primarily through this kind of processes. This result can explain why $X(1870)$ has been first observed in the $\eta\pi\pi$ channel.

Thirdly, the two-body strong decay of $X(1870)$ is computed in the $^3P_0$ model. As the $\eta_2(2^1D_2)$ quarkonium, the predicted width of $X(1870)$ looks much larger than the observations. The broad resonance, $\eta_2(1870)$, can be a natural candidate for the $2^1D_2 n\bar{n}$ meson. There, we fix the creation strength, γ, in two kinds of processes: (1) $n\bar{n} \to n\bar{n}+n\bar{n}$; (2) $n\bar{n} \to n\bar{s}+s\bar{n}$ and $s\bar{s} \to n\bar{s}+s\bar{n}$. The functions of creation

vertex are determined as $\gamma(p) = 3.0 + 25\exp(-4p^2)$ and $\gamma(p) = 1.8 + 4\exp(-10p^2)$, respectively. Meanwhile, the SHO wave function scale, βs, is obtained by the GI potential model.

We have evaluated the magnitude of the partial widths of "$\mathcal{S} + P$" channels by the ratio, $(\Gamma(X(1870) \to a_0(980)\pi))/(\Gamma(\eta(1295) \to a_0(980)\pi))$, under a rather crude assumption that $\eta(1295)/X(1870) \to a_0(980)\pi$ through a virtual intermediate $1\,^3P_0 q\bar{q}$ meson (see Figure 7). Then the uncertainties of the coupling vertex for $1\,^3P_0(q\bar{q}) \to a_0(980)$ are assumed to be canceled in the ratio. The total widths of "$\mathcal{S} + P$" are evaluated no more than 12.6 MeV and $\Gamma(X(1870) \to a_0(980)\pi) \leq 3.8$ MeV. Since $X(1870)$ primarily decays via $a_0(980)\pi$, it also indicated that the $X(1870)$ cannot be interpreted as the $2^1D_2 n\bar{n}$ state.

We also study the $X(1870)$ as a hybrid state in the flux tube model. Our results agree well with most of predictions given by [16]. $X(1870)$ looks most like the $\eta_H(0^+2^{-+})$ state for the narrow predicted width, which is consistent with the experiments. But we cannot exclude the possibility of 0^+1^{++}. A precise measurement of $a_1(1260)\pi$ is suggested to pin down this uncertainty.

Finally, some important arguments and useful suggestions are given as follows. (1) If $\eta_2(1870)$ is the $\eta_2(2^1D_2)$ state, the broad $\pi_2(1880)$ should be isovector partner of $\eta_2(1870)$. $\pi_2(1880)$ has been interpreted as the conventional 2^1D_2 $q\bar{q}$ meson in [76]. Indeed, the decay channel of $\omega\rho$ is large enough for $\pi_2(1880)$ [77]. This observation disfavors the $\pi_2(1880)$ as a 2^{-+} hybrid candidate for the selection rule that a hybrid meson decaying into two S-wave mesons is strongly suppressed [78]. (2) If $X(1870)$ is a hybrid meson, we suggest to search its isospin partner in the decay channels of $J/\psi \to \rho f_0(980)\pi$ and $J/\psi \to \rho b_1(1235)\pi$, which are accessible at BESIII, Belle, and BABAR Collaborations. The decay channel of $b_1(1235)\pi$ is forbidden for the $\pi_2(2^1D_2)$ quarkonium due to the "spin selection rule" [60, 79]. We also suggest to search the $\eta_2(1870)$ in the decay channels of $J/\psi \to \gamma\rho\rho$ and $J/\psi \to \gamma\omega\omega$ since these channels are forbidden for the hybrid production.

Appendices

A. The Expressions of Amplitudes

We have omitted an exponential factor in the following decay amplitudes $\mathcal{M}_{LS}$ for compactness:

$$\exp\left(-\frac{2\lambda\mu - \nu^2}{4\mu}p^2\right), \tag{A.1}$$

where we defined

$$\mu = \frac{1}{2}\left(\frac{1}{\beta_A^2} + \frac{1}{\beta_B^2} + \frac{1}{\beta_C^2}\right),$$
$$\nu = \frac{m_1}{(m+m_1)\beta_B^2} + \frac{m_2}{(m+m_2)\beta_C^2},$$
$$\lambda = \frac{m_1^2}{(m+m_1)^2\beta_B^2} + \frac{m_2^2}{(m+m_2)^2\beta_C^2}, \qquad \eta = \frac{m_1}{m+m_1}. \tag{A.2}$$

For $1^3S_1 \to 1^1S_0 + 1^1S_0$,

$$\mathcal{M}_{10} = \frac{2\mu - \nu}{8\sqrt{3}\pi^{5/4}\mu^{5/2}(\beta_A\beta_B\beta_C)^{3/2}}p. \tag{A.3}$$

For $1^3P_2 \to 1^1S_0 + 1^1S_0$,

$$\mathcal{M}_{20} = \frac{2\mu\beta_B^{3/2} - \left(p^2\nu^2 + 2\mu\left(1 - p^2\nu\right)\right)\beta_C^{3/2}}{8\sqrt{15}\pi^{5/4}\mu^{7/2}\beta_A^{5/2}\beta_B^{3/2}\beta_C^3}. \tag{A.4}$$

For $1^3P_2 \to 1^3S_1 + 1^1S_0$, $\mathcal{M}_{21} = -\sqrt{3/2}\mathcal{M}_{20}$.
For $1^3P_1 \to 1^3S_1 + 1^1S_0$,

$$\mathcal{M}_{01} = \frac{4\mu\beta_B^{3/2} + \left(p^2\nu^2 + 2\mu\left(1 - p^2\nu\right)\right)\beta_C^{3/2}}{24\pi^{5/4}\mu^{7/2}\beta_A^{5/2}\beta_B^{3/2}\beta_C^3},$$
$$\mathcal{M}_{21} = \frac{(2\mu - \nu)\nu}{24\sqrt{2}\pi^{5/4}\mu^{7/2}\beta_A^{5/2}\beta_B^{3/2}\beta_C^3}p^2. \tag{A.5}$$

For $1^3D_3 \to 1^1S_0 + 1^1S_0$,

$$\mathcal{M}_{30} = -\frac{2\mu - \nu}{16\sqrt{35}\pi^{5/4}\mu^{9/2}\beta_A^{9/2}\beta_B^{3/2}\beta_C^{3/2}}\nu^2p^3. \tag{A.6}$$

For $2^1S_0 \to 1^3P_0 + 1^1S_0$,

$$\begin{aligned}\mathcal{M}_{11} = {} & \frac{1}{96\pi^{5/4}\mu^{11/2}\beta_A^{7/2}\beta_B^{5/2}\beta_C^{3/2}} \\ & \times\Big(-24p^2\eta\mu^3 - p^4\nu^4 + 2p^2\mu\nu^2\left(-10 + p^2(1+\eta)\nu\right) \\ & - 4\mu^2\left(15 - 5p^2(1+\eta)\nu + p^4\eta\nu^2\right) + 6\mu^2 \\ & \times\left(4p^2\eta\mu^2 + p^2\nu^2 - 2\mu\left(-3 + p^2(1+\eta)\nu\right)\right)\beta_A^2\Big).\end{aligned} \tag{A.7}$$

For $2^1D_2 \to 1^3S_1 + 1^1S_0$,

$$\begin{aligned}\mathcal{M}_{11} = {} & \Big(\Big(-p^4\nu^4 + 2p^2\nu^2\mu\left(\nu p^2 - 14\right) + 28\mu^2\left(\nu p^2 - 5\right) \\ & + 14\mu^2\left(p^2\nu^2 - 2\left(\nu p^2 - 5\right)\mu\beta_A^2\right)\Big) \\ & \times\left(160\sqrt{21}\pi^{5/4}\mu^{13/2}\beta_A^{11/2}\beta_B^{3/2}\beta_C^{3/2}\right)^{-1}\Big)\nu p, \\ \mathcal{M}_{31} = {} & \Big(\Big(-28\mu^2 + \nu^3p^2 - 2\mu\nu\left(\nu p^2 - 9\right) \\ & + 14(2\mu - \nu)\mu^2\beta_A^2\Big) \\ & \times\left(160\sqrt{14}\pi^{5/4}\mu^{13/2}\beta_A^{11/2}\beta_B^{3/2}\beta_C^{3/2}\right)^{-1}\Big) \times \nu^2p^3.\end{aligned} \tag{A.8}$$

For $2^1D_2 \to 1^3S_1 + 1^3S_1$, $\mathcal{M}'_{11} = \sqrt{2}\mathcal{M}_{11}$ and $\mathcal{M}'_{31} = \sqrt{2}\mathcal{M}_{31}$.

For $2^1D_2 \rightarrow 1^3P_0 + 1^1S_0$

$$\begin{aligned}\mathscr{M}_{20} = & -\frac{1}{192\sqrt{35}\pi^{5/4}\mu^{15/2}\beta_A^{11/2}\beta_B^{5/2}\beta_C^{3/2}} \\ & \times\left(p^4\nu^5 - 2p^2\mu\nu^3\left(-18 + p^2(1+\eta)\nu\right)\right. \\ & + 4\mu^2\nu\left(63 - 11p^2(1+\eta)\nu + p^4\eta\nu^2\right) \\ & + 56\mu^3\left(-2 + \eta\left(-2 + p^2\nu\right)\right) \\ & - 14\mu^2\left(p^2\nu^3 - 2\mu\nu\left(-7 + p^2(1+\eta)\nu\right)\right. \\ & \left.\left.+4\mu^2\left(-2 + \eta\left(-2 + p^2\nu\right)\right)\right)\beta_A^2\right)\nu p^2.\end{aligned} \tag{A.9}$$

For $2^1D_2 \rightarrow 1^3P_1 + 1^1S_0$,

$$\begin{aligned}\mathscr{M}_{21} = & -\frac{p^2\nu^2 - 14\mu^2\beta_A^2 + 14\mu}{16\sqrt{35}\pi^{5/4}\mu^{11/2}\beta_A^{11/2}\beta_B^{5/2}\beta_C^{3/2}} \\ & \times(\eta - 1)\nu p^2.\end{aligned} \tag{A.10}$$

For $2^1D_2 \rightarrow 1^3P_2 + 1^1S_0$,

$$\begin{aligned}\mathscr{M}_{02} = & \frac{1}{480\sqrt{14}\pi^{5/4}\mu^{15/2}\beta_A^{11/2}\beta_B^{5/2}\beta_C^{3/2}} \\ & \times\left(p^6\mu^6 - 2p^4\mu\nu^4\left(p^2(1+\eta)\nu - 21\right)\right. \\ & + 4p^2\mu^2\nu^2\left(105 - 14p^2(1+\eta)\nu + p^4\eta\nu^2\right) \\ & + 56\mu^3\left(15 - 5p^2(1+\eta)\nu + p^4\eta\nu^2\right) \\ & - 14\mu^2\left(p^4\nu^4 - 2p^2\mu\nu^2\left(-10 + p^2(1+\eta)\nu\right)\right. \\ & \left.\left.+ 4\mu^2\left(15 - 5p^2(1+\eta)\nu + p^4\eta\nu^2\right)\right)\beta_A^2\right), \\ \mathscr{M}_{22} = & -\frac{1}{672\sqrt{5}\pi^{5/4}\mu^{15/2}\beta_A^{15/2}\beta_B^{5/2}\beta_C^{3/2}} \\ & \times\left(p^4\nu^5 - 2p^2\mu\nu^3\left(-18 + p^2(1+\eta)\nu\right)\right. \\ & + 2\mu^2\nu\left(126 - 25p^2(1+\eta)\nu + 2p^4\eta\nu^2\right) \\ & + 28\mu^3\left(-7 + \eta\left(-7 + 2p^2\nu\right)\right) \\ & - 14\left(\mu^2\right)\left(p^2\nu^3 - 2\mu\nu\left(-7 + p^2(1+\eta)\nu\right)\right. \\ & \left.\left.+ 2\mu^2\left(-7 + \eta\left(-7 + 2p^2\nu\right)\right)\right)\beta_A^2\right)\nu p^2, \\ \mathscr{M}_{42} = & -\frac{1}{1120\pi^{5/4}\mu^{15/2}\beta_A^{11/2}\beta_B^{5/2}\beta_C^{3/2}} \\ & \times\left(\nu\left(p^2\nu^3 - 36\mu^2 + 2\mu\nu\left(11 - p^2\nu\right)\right)\right. \\ & + 2\eta\mu\left(28\mu^2 - p^2\nu^3 + 2\mu\nu\left(p^2\nu - 9\right)\right) \\ & \left.-14\mu^2(2\mu - \nu)(2\eta\mu - \nu)\beta_A^2\right)\nu^2p^4.\end{aligned} \tag{A.11}$$

For $2^1D_2 \rightarrow 2^3P_1 + 1^1S_0$

$$\begin{aligned}\mathscr{M}_{21} = & \frac{1}{160\sqrt{14}\pi^{5/4}\mu^{15/2}\beta_A^{11/2}\beta_B^{9/2}\beta_C^{3/2}} \\ & \times\left(-112\eta\mu^3 + 252\mu^2\nu + 56p^2\eta^2\mu^3\nu\right. \\ & - 80p^2\eta\mu^2\nu^2 + 36p^2\mu\nu^3 \\ & + 4p^4\eta^2\mu^2\nu^3 - 4p^4\eta\mu\nu^4 + p^4\nu^5 \\ & - 10\mu^2\nu\left(14\mu + p^2\nu^2\right)\beta_B^2 \\ & - 14\mu^2\beta_A^2\left(14\mu\nu + 4p^2\eta^2\mu^2\nu + p^2\nu^3\right. \\ & \left.\left.- 4\eta\mu\left(2\mu + p^2\nu^2\right) - 10\mu^2\nu\beta_B^2\right)\right) \\ & \times(\eta - 1)p^2.\end{aligned} \tag{A.12}$$

m_1 and m_2 are the masses of quarks in the decaying meson A. m is the mass of the created quark from the vacuum. For calculating the decay widths, the masses of quarks are taken as $m_u = m_d = 0.220\,\text{GeV}$, $m_s = 0.428\,\text{GeV}$, which are the same as those in Section 2. The above amplitudes, $\mathscr{M}_{LS}$, can be reduced further in the approximation of $m_1 = m_2 = m$ and $\beta_A = \beta_B = \beta_C = \beta$. The reduced $\mathscr{M}_{LS}$ are consistent with those given by [71] except for an unimportant factor, $-2^{9/2}$, since this factor can be absorbed into the coefficient γ.

B. Hybrid Decay in the Flux Tube Model

The flux tube model was motivated by the strong coupling expansion of the lattice QCD. In this model, decay occurs when the flux-tube breaks at any point along its length, with a $q\bar{q}$ pair production in a relative $J^{PC} = 0^{++}$ state. It is similar to the $^3P_0$ decay model but with an essential difference. The flux tube model extends the nonrelativistic constituent quark model to include gluonic degrees of freedom in a very simple and intuitive way, where the gluonic field is regarded as tubes of color flux. Then it can be extended to the hybrid research. When the hybrid mesons are assumed to be narrow, and the threshold effects are not taken into account, the partial decay width $\Gamma_{LS}(H \rightarrow BC)$ is given by the flux model as [79]

$$\Gamma_{LS}(H \longrightarrow BC) = \frac{p}{(2J_A + 1)\pi}\frac{\widetilde{M}_B\widetilde{M}_C}{\widetilde{M}_A}\left|\mathscr{M}_{LS}(H \longrightarrow BC)\right|^2, \tag{B.1}$$

where $\widetilde{M}_A$, $\widetilde{M}_B$, $\widetilde{M}_C$ are the "mock-meson" masses of A, B, C [64]. When a hybrid meson decays into P-wave and

Table 9: Partial wave amplitudes $\widetilde{\mathscr{M}}_L(H \to BC)$ for an initial hybrid H decaying into a P-wave and pseudoscalar mesons.

B	$H(0^+0^{-+})$	$H(0^+1^{++})$	$H(0^+2^{-+})$
0^{++}	$+\sqrt{2}\mathscr{M}_S/3$	$-\sqrt{2}\mathscr{M}_{P_2}/\sqrt{3}$	$+\mathscr{M}_D/3$
1^{++}	—	$-\mathscr{M}_{P_1}/\sqrt{2}$	—
2^{++}	$+\mathscr{M}_D/3$	$-\mathscr{M}_{P_4}/\sqrt{30}$	$-\sqrt{5}\mathscr{M}_S/\sqrt{18}$
		$+\mathscr{M}_F/\sqrt{5}$	$-\sqrt{7}\mathscr{M}_D/3$

pseudoscalar mesons, the partial wave amplitude $\mathscr{M}_L(H \to BC)$ (with $S = S_B$) is given as the following form:

$$\begin{aligned}\mathscr{M}_L&(H \longrightarrow BC)\\ &= \langle \phi_B\phi_C \mid \phi_A\phi_0\rangle \left(\frac{a\tilde{c}}{9\sqrt{3}}\frac{1}{2}A^0_{00}\sqrt{\frac{fb}{\pi}}\right)\frac{\kappa\sqrt{b}}{\left(1+fb/(2\tilde{\beta}^2)\right)^2}\\ &\quad\times\sqrt{\frac{2\pi}{3\Gamma\left(\frac{3}{2}+\delta\right)}}\frac{\beta_A^{3/2+\delta}}{\tilde{\beta}}\widetilde{\mathscr{M}}_L(H \longrightarrow BC).\end{aligned} \tag{B.2}$$

The flavor matrix element $\langle \phi_B\phi_C \mid \phi_A\phi_0\rangle$ has been discussed before. $\widetilde{\mathscr{M}}_L(H \to BC)$ are listed in Table 9 for the states of $\eta_H(0^+0^{-+})$, $f_H(0^+1^{++})$, and $\eta_H(0^+2^{-+})$.

Here the $\mathscr{M}_S$, $\mathscr{M}_D$, $\mathscr{M}_{P_i}$, and $\mathscr{M}_F$ are defined as $\mathscr{M}_S = -(3\tilde{h}_0 - \tilde{g}_1 + 4\tilde{h}_2)$, $\mathscr{M}_D = (\tilde{g}_1 + 5\tilde{h}_2)$, $\mathscr{M}_{P_1} = -i(2\tilde{g}_0 + 3\tilde{h}_1 - \tilde{g}_2)$, $\mathscr{M}_{P_2} = -i(\tilde{g}_0 + \tilde{g}_2)$, $\mathscr{M}_{P_4} = -i(10\tilde{g}_0 + 9\tilde{h}_1 + \tilde{g}_2)$, and $\mathscr{M}_F = -3i(\tilde{g}_2 + \tilde{h}_3)$. The analytical expressions of $\tilde{g}_i$ and $\tilde{h}_i$ are given as

$$\begin{aligned}\tilde{g}_n &= 2^{3+\delta}\frac{M^n m}{(M+m)^{n+1}}\left(2\beta_A^2+\tilde{\beta}^2\right)^{-(n+\delta+3)/2}\Gamma\left(\frac{n+\delta+3}{2}\right)_1\\ &\quad\times F_1\left[\frac{n+\delta+3}{2}, n+1, -\left(\frac{M}{M+m}\right)^2\right.\\ &\qquad\left.\times\frac{p^2}{2\beta_A^2+\tilde{\beta}^2}\right]p^{n+1},\\ \tilde{h}_n &= 2^{3+\delta}\tilde{\beta}^2\left(\frac{M}{M+m}\right)^n\left(2\beta_A^2+\tilde{\beta}^2\right)^{-(n+\delta+4)/2}\Gamma\left(\frac{n+\delta+4}{2}\right)_1\\ &\quad\times F_1\left[\frac{n+\delta+4}{2}, n+1, -\left(\frac{M}{M+m}\right)^2\frac{p^2}{2\beta_A^2+\tilde{\beta}^2}\right]p^n,\end{aligned} \tag{B.3}$$

where ${}_1F_1[\cdot]$ are the confluent hypergeometric functions. Here we do not take account of the decay channels of $H \to 2S + 1S$ because they are forbidden by the conservation laws, or the "spin selection rule," or the phase space; for example, the decay channel of $\pi(1300) + \pi$ is forbidden for the $f_H(0^+1^{++})$ state by the "spin selection rule." In this work, we choose to follow [79] and take the combination $(a\tilde{c}/9\sqrt{3})(1/2)A^0_{00}\sqrt{fb/\pi}$ as 0.64 which was fixed by the conventional mesons [64], $M = m = m_{u,d} = 330$ MeV, $\widetilde{M}_B^{I=0} = \widetilde{M}_B^{I=1} = 1250$ MeV, $\widetilde{M}_C^{I=0} = 720$ MeV, $\widetilde{M}_C^{I=1} = 850$ MeV, $\beta_A = 0.27$ GeV, $\delta = 0.62$, $b = 0.18$ GeV^2, and $\kappa = 0.9$. Final states containing π have $\tilde{\beta} = 0.36$ GeV; otherwise $\tilde{\beta} = 0.40$ GeV.

Acknowledgments

Bing Chen thanks Jun-Long Tian and D. V. Bugg for very helpful discussions. This work is supported by the Key Program of the He'nan Educational Committee of China (nos. 13A140014 and 12B140001), the National Natural Science Foundation of China under Grant no. 11305003, 11075102, 11005003, and U1204115, the Innovation Program of Shanghai Municipal Education Commission under Grant no. 13ZZ066, and the Program of He'nan Technology Department (no. 11147201).

References

[1] M. Ablikim, M. N. Achasov, D. Alberto et al., "$\eta\pi^+\pi^-$ Resonant Structure around 1. 8 GeV/c^2 and $\eta(1405)$ in $J/\psi \to \omega\eta\pi^+\pi^-$," *Physical Review Letters*, vol. 107, no. 18, Article ID 182001, 2011.

[2] J. Beringer, J. F. Arguin, R. M. Barnett et al., "Review of particle physics," *Physical Review D*, vol. 86, no. 1, Article ID 010001, 2012.

[3] K. Karch, D. Antreasyan, H. W. Bartels et al., "Analysis of the $\eta\pi^0\pi^0$ final state in photon-photon collisions," *Zeitschrift für Physik C*, vol. 54, no. 1, pp. 33–44, 1992.

[4] M. Feindt, DESY-90-128 (1990), to appear in Proceedings of the 25th International Conference on High Energy Physics, Singapore 1990.

[5] J. Adomeit, C. Amsler, D. S. Armstrong et al., "Evidence for two isospin zero $J^{PC} = 2^{-+}$ mesons at 1645 and 1875 MeV," *Zeitschrift für Physik C*, vol. 71, no. 1, pp. 227–238, 1996.

[6] A. V. Anisovich, C. A. Baker, C. J. Batty et al., "Three $I = 0J^{PC} = 2^{-+}$ mesons," *Physics Letters B*, vol. 477, no. 1–3, pp. 19–27, 2000.

[7] D. Barberis, F. G. Binon, F. E. Close et al., "A study of the $\eta\pi^+\pi^-$ channel produced in central pp interactions at 450 GeV/c^2," *Physics Letters B*, vol. 471, no. 4, pp. 435–439, 2000.

[8] D. Barberis, F. G. Binon, F. E. Close, and K. M. Danielsen, "A spin analysis of the 4π channels produced in central pp interactions at 450 GeV/c^2," *Physics Letters B*, vol. 471, no. 4, pp. 440–448, 2000.

[9] J. Z. Bai, Y. Ban, and J. G. Bian, "Partial wave analysis of $J/\psi \to \gamma(\eta\pi^+\pi^-)$," *Physics Letters B*, vol. 446, no. 3, pp. 356–362, 1999.

[10] A. V. Anisovich, C. J. Batty, D. V. Bugg et al., "A fresh look at $\eta_2(1645)$, $\eta_2(1870)$, $\eta_2(2030)$ and $f_2(1910)$ in $\bar{p}p \to \eta\pi^0\pi^0\pi^0$," *The European Physical Journal C*, vol. 71, Article ID 1511, 2011.

[11] M. Chanowitz and S. Sharpe, "Hybrids: mixed states of quarks and gluons," *Nuclear Physics, Section B*, vol. 222, no. 2, pp. 211–244, 1983.

[12] T. Barnes, F. E. Close, and F. de Viron, "$Q\bar{Q}g$ hybrid mesons in the MIT bag model," *Nuclear Physics, Section B*, vol. 224, no. 2, pp. 241–264, 1983.

[13] N. Isgur and J. Paton, "Flux-tube model for hadrons in QCD," *Physical Review D*, vol. 31, no. 11, pp. 2910–2929, 1985.

[14] T. Barnes, F. E. Close, and E. S. Swanson, "Hybrid and conventional mesons in the flux tube model: numerical studies and their phenomenological implications," *Physical Review D*, vol. 52, no. 9, pp. 5242–5256, 1995.

[15] S. Ishida, H. Sawazaki, M. Oda, and K. Yamada, "Decay properties of hybrid mesons with a massive constituent gluon and search for their candidates," *Physical Review D*, vol. 47, no. 1, pp. 179–198, 1993.

[16] P. R. Page, E. S. Swanson, and A. P. Szczepaniak, "Hybrid meson decay phenomenology," *Physical Review D*, vol. 59, no. 3, pp. 1–19, 1999.

[17] C. J. Morningstar and M. Peardon, "Glueball spectrum from an anisotropic lattice study," *Physical Review D*, vol. 60, no. 3, pp. 1–13, 1999.

[18] Y. Chen, A. Alexandru, S. J. Dong et al., "Glueball spectrum and matrix elements on anisotropic lattices," *Physical Review D*, vol. 73, no. 1, 2006.

[19] E. Gregory, A. Irving, B. Lucini et al., "Towards the glueball spectrum from unquenched lattice QCD," *Journal of High Energy Physics*, vol. 10, p. 170, 2012.

[20] S. Godfrey and N. Isgur, "Mesons in a relativized quark model with chromodynamics," *Physical Review D*, vol. 32, no. 1, pp. 189–231, 1985.

[21] D. V. Bugg, "Four sorts of meson," *Physics Reports*, vol. 397, no. 5, pp. 257–358, 2004.

[22] E. Klempt and A. Zaitsev, "Glueballs, hybrids, multiquarks. Experimental facts versus QCD inspired concepts," *Physics Reports*, vol. 454, no. 1–4, pp. 1–202, 2007.

[23] C. Amsler and F. E. Close, "Is $f_0(1500)$ a scalar glueball?" *Physical Review D*, vol. 53, no. 1, pp. 295–311, 1996.

[24] D.-M. Li and E. Wang, "Canonical interpretation of the $\eta_2(1870)$," *European Physical Journal C*, vol. 63, no. 2, pp. 297–304, 2009.

[25] D. Ebert, R. N. Faustov, and V. O. Galkin, "Mass spectra and Regge trajectories of light mesons in the relativistic quark model," *Physical Review D*, vol. 79, no. 11, Article ID 114029, 2009.

[26] R. Giachetti and E. Sorace, "Unified covariant treatment of hyperfine splitting for heavy and light mesons," *Physical Review D*, vol. 87, no. 3, Article ID 034021, 2013.

[27] J. Vijande, F. Fernández, and A. Valcarce, "Constituent quark model study of the meson spectra," *Journal of Physics G*, vol. 31, no. 5, pp. 481–506, 2005.

[28] R. Bonnaz and B. Silvestre-Brac, "Discussion of the $^3P_0$ model applied to the decay of mesons into two mesons," *Few-Body Systems*, vol. 27, no. 3-4, pp. 163–187, 1999.

[29] E. Eichten, K. Gottfried, T. Kinoshita, J. Kogut, K. D. Lane, and T.-M. Yan, "Spectrum of charmed quark-antiquark bound states," *Physical Review Letters*, vol. 34, no. 6, pp. 369–372, 1975.

[30] A. M. Badalian and B. L. G. Bakker, "Nonperturbative hyperfine contribution to the b1 and h1 meson masses," *Physical Review D*, vol. 64, no. 11, Article ID 114010, 2001.

[31] S. Dobbs, Z. Metreveli, K. K. Seth et al., "Precision measurement of the mass of the $h_c(^1P_1)$ state of charmonium," *Physical Review Letters*, vol. 101, no. 18, Article ID 182003, 2008.

[32] D. S. Hwang, C. S. Kim, and W. Namgung, "Dependence of $|V_{ub}/V_{cb}|$ on Fermi momentum P_f in ACCMM model," *Zeitschrift für Physik C*, vol. 69, no. 1, pp. 107–112, 1995.

[33] S. F. Radford, W. W. Repko, and M. J. Saelim, "Potential model calculations and predictions for $c\bar{c}$ quarkonia," *Physical Review D*, vol. 80, no. 3, Article ID 034012, 2009.

[34] S. F. Radford and W. W. Repko, "Potential model calculations and predictions for heavy quarkonium," *Physical Review D*, vol. 75, no. 7, Article ID 074031, 2007.

[35] W. Roberts and B. Silvestre-Brac, "Meson decays in a quark model," *Physical Review D*, vol. 57, no. 3, pp. 1694–1702, 1998.

[36] T. Barnes, S. Godfrey, and E. S. Swanson, "Higher charmonia," *Physical Review D*, vol. 72, no. 5, Article ID 054026, 2005.

[37] A. M. Badalian, B. L. G. Bakker, and Y. A. Simonov, "Light meson radial Regge trajectories," *Physical Review D*, vol. 66, no. 3, Article ID 034026, 2002.

[38] S. Godfrey and R. Kokoski, "Properties of P-wave mesons with one heavy quark," *Physical Review D*, vol. 43, no. 5, pp. 1679–1687, 1991.

[39] F. E. Close and E. S. Swanson, "Dynamics and decay of heavy-light hadrons," *Physical Review D*, vol. 72, no. 9, Article ID 094004, 2005.

[40] D.-M. Li, P.-F. Ji, and B. Ma, "The newly observed open-charm states in quark model," *The European Physical Journal C*, vol. 71, no. 3, Article ID 1582, 2011.

[41] P. González, "Long-distance behavior of the quark-antiquark static potential. Application to light-quark mesons and heavy quarkonia," *Physical Review D*, vol. 80, no. 5, Article ID 054010, 2009.

[42] D.-M. Li and B. Ma, "$X(1835)$ and $\eta(1760)$ observed by the BES Collaboration," *Physical Review D*, vol. 77, no. 7, Article ID 074004, 2008.

[43] J.-F. Liu, G.-J. Ding, and M.-L. Yan, "$X(1835)$ and the new resonances $X(2120)$ and $X(2370)$ observed by the BES collaboration," *Physical Review D*, vol. 82, no. 7, Article ID 074026, 2010.

[44] J.-S. Yu, Z.-F. Sun, X. Liu, and Q. Zhao, "Categorizing resonances $X(1835)$, $X(2120)$, and $X(2370)$ in the pseudoscalar meson family," *Physical Review D*, vol. 83, no. 11, Article ID 114007, 2011.

[45] P. Masjuan, E. R. Arriola, and W. Broniowski, "Systematics of radial and angular-momentum Regge trajectories of light nonstrange $\bar{p}p$-states," *Physical Review D*, vol. 85, no. 9, Article ID 094006, 2012.

[46] D. V. Bugg, "Comment on 'Systematics of radial and angular-momentum Regge trajectories of light nonstrange $\bar{p}p$-states,'" *Physical Review D*, vol. 87, no. 11, Article ID 118501, 2013.

[47] P. Masjuan, E. R. Arriola, and W. Broniowski, "Reply to 'Comment on "Systematics of radial and angular-momentum Regge trajectories of light nonstrange $\bar{p}p$-states"'," *Physical Review D*, vol. 87, no. 11, Article ID 118502, 2013.

[48] L. Maiani, F. Piccinini, A. D. Polosa, and V. Riquer, "New look at scalar mesons," *Physical Review Letters*, vol. 93, no. 21, Article ID 212002, 2004.

[49] J. Weinstein and N. Isgur, "Do multiquark hadrons exist?" *Physical Review Letters*, vol. 48, no. 10, pp. 659–662, 1982.

[50] J. Weinstein and N. Isgur, "qqqq—system in a potential model," *Physical Review D*, vol. 27, no. 3, pp. 588–599, 1983.

[51] J. Weinstein and N. Isgur, "$K\bar{K}$ molecules," *Physical Review D*, vol. 41, no. 7, pp. 2236–2257, 1990.

[52] R. L. Jaffe, "Multiquark hadrons. II. Methods," *Physical Review D*, vol. 15, no. 1, pp. 281–289, 1977.

[53] R. L. Jaffe and F. E. Low, "Connection between quark-model eigenstates and low-energy scattering," *Physical Review D*, vol. 19, no. 7, pp. 2105–2118, 1979.

[54] M. Alford and R. L. Jaffe, "Insight into the scalar mesons from a lattice calculation," *Nuclear Physics B*, vol. 578, no. 1-2, pp. 367–382, 2000.

[55] Z.-G. Luo, X.-L. Chen, and X. Liu, "$B_{s1}(5830)$ and $B^*_{s1}(5840)$," *Physical Review D*, vol. 79, no. 7, Article ID 074020, 2009.

[56] R. L. Jaffe, "Exotica," *Physics Reports*, vol. 409, no. 1, pp. 1–45, 2005.

[57] A. Selem and F. Wilczek, "Hadron Systematics and Emergent Diquarks," Talk by FW at a workshop at Schloss Ringberg, October 2005, http://arxiv.org/abs/hep-ph/0602128.

[58] E. Santopinto and G. Galatà, "Spectroscopy of tetraquark states," *Physical Review C*, vol. 75, no. 4, Article ID 045206, 2007.

[59] J. J. De Swart, "The octet model and its clebsch-gordan coefficients," *Reviews of Modern Physics*, vol. 35, no. 4, pp. 916–939, 1963.

[60] T. J. Burns, F. E. Close, and C. E. Thomas, "Dynamics of hadron strong production and decay," *Physical Review D*, vol. 77, no. 3, Article ID 034008, 2008.

[61] L. Micu, "Decay rates of meson resonances in a quark model," *Nuclear Physics B*, vol. 10, no. 3, pp. 521–526, 1969.

[62] A. Le Yaouanc, L. Oliver, O. Pène, and J.-C. Raynal, ""naive" quark-pair-creation model of strong-interaction vertices," *Physical Review D*, vol. 8, no. 7, pp. 2223–2234, 1973.

[63] A. Le Yaouanc, L. Oliver, O. Pene, and J. C. Raynal, *Hadron Transition in the Quark Model*, Gordon and Breach, New York, NY, USA, 1988.

[64] R. Kokoski and N. Isgur, "Meson decays by flux-tube breaking," *Physical Review D*, vol. 35, no. 3, pp. 907–933, 1987.

[65] E. S. Ackleh, T. Barnes, and E. S. Swanson, "On the mechanism of open-flavor strong decays," *Physical Review D*, vol. 54, no. 11, pp. 6811–6829, 1996.

[66] J. Segovia, D. R. Entem, and F. Fernandez, "Scaling of the $^3P_0$ strength in heavy meson strong decays," *Physics Letters B*, vol. 715, no. 4, pp. 322–327, 2012.

[67] C. Hayne and N. Isgur, "Beyond the wave function at the origin: some momentum-dependent effects in the nonrelativistic quark model," *Physical Review D*, vol. 25, no. 7, pp. 1944–1950, 1982.

[68] M. Jacob and G. C. Wick, "On the general theory of collisions for particles with spin," *Annals of Physics*, vol. 7, no. 4, pp. 404–428, 1959.

[69] P. Geiger and E. S. Swanson, "Distinguishing among strong decay models," *Physical Review D*, vol. 50, no. 11, pp. 6855–6862, 1994.

[70] H. G. Blundel, "Meson properties in the Quark model: a look at some outstanding problems," http://arxiv.org/abs/hep-ph/9608473.

[71] T. Barnes, F. E. Close, P. R. Page, and E. S. Swanson, "Higher quarkonia," *Physical Review D*, vol. 55, no. 7, pp. 4157–4188, 1997.

[72] R. M. Baltrusaitis, D. Coffman, J. Hauser et al., "Study of the radiative decay $J/\psi \to \gamma\rho\rho$," *Physical Review D*, vol. 33, no. 5, pp. 1222–1232, 1986.

[73] R. M. Baltrusaitis, J. J. Becker, G. T. Blaylock et al., "Observation of J/ψ radiative decay to pseudoscalar $\omega\omega$," *Physical Review Letters*, vol. 55, no. 17, pp. 1723–1726, 1985.

[74] M. Ablikim, J. Z. Bai, Y. Ban et al., "Pseudoscalar production at threshold in $J/\psi \to \gamma\omega\omega$," *Physical Review D*, vol. 73, no. 11, Article ID 112007, 2006.

[75] N. Isgur, R. Kokoski, and J. Paton, "Gluonic excitations of mesons: why they are missing and where to find them," *Physical Review Letters*, vol. 54, no. 9, pp. 869–872, 1985.

[76] D.-M. Li and S. Zhou, "Nature of the $\pi_2(1880)$," *Physical Review D*, vol. 79, no. 1, Article ID 014014, 2009.

[77] M. Lu, G. S. Adams, T. Adams et al., "Exotic Meson decay to $\omega\pi^0\pi^-$," *Physical Review Letters*, vol. 94, no. 3, Article ID 032002, 2005.

[78] P. R. Page, "Why hybrid meson coupling to two S-wave mesons is suppressed," *Physics Letters B*, vol. 402, no. 1-2, pp. 183–188, 1997.

[79] F. E. Close and P. R. Page, "The production and decay of hybrid mesons by flux-tube breaking," *Nuclear Physics B*, vol. 443, no. 1-2, pp. 233–254, 1995.